

## Research Letter

# Using $^{18}\text{F}$ -DCFPyL Prostate-Specific Membrane Antigen–Directed Positron Emission Tomography/Magnetic Resonance Imaging to Define Intraprostatic Boosts for Prostate Stereotactic Body Radiation Therapy



John M. Floberg, MD, PhD,<sup>a,\*</sup> Shane A. Wells, MD,<sup>b</sup> Diane Ojala, CMD,<sup>c</sup> R. Adam Bayliss, PhD,<sup>a</sup> Patrick M. Hill, PhD,<sup>a</sup> Brett A. Morris, MD, PhD,<sup>a</sup> Zachary S. Morris, MD, PhD,<sup>a</sup> Mark Ritter, MD, PhD,<sup>a</sup> and Steve Y. Cho, MD<sup>b</sup>

<sup>a</sup>Departments of Human Oncology; <sup>b</sup>Radiology, University of Wisconsin, Madison, Wisconsin; and <sup>c</sup>Radiation Oncology, UW Health, Madison, Wisconsin

Received 9 September 2022; accepted 29 March 2023

**Purpose:** The recently reported FLAME trial demonstrated a biochemical disease-free survival benefit to using a focal intraprostatic boost to multiparametric magnetic resonance imaging (mpMRI)–identified lesions in men with localized prostate cancer treated with definitive radiation therapy. Prostate-specific membrane antigen (PSMA)–directed positron emission tomography (PET) may identify additional areas of disease. In this work, we investigated using both PSMA PET and mpMRI in planning focal intraprostatic boosts using stereotactic body radiation therapy (SBRT).

**Methods and Materials:** We evaluated a cohort of patients (n = 13) with localized prostate cancer who were imaged with 2-(3-(1-carboxy-5-[(6-[ $^{18}\text{F}$ ]fluoro-pyridine-2-carbonyl)-amino]-pentyl)-ureido)-pentanedioic acid ( $^{18}\text{F}$ -DCFPyL) PET/MRI on a prospective imaging trial before undergoing definitive therapy. The number of lesions concordant (overlapping) and discordant (no overlap) on PET and MRI was assessed. Overlap between concordant lesions was evaluated using the Dice and Jaccard similarity coefficients. Prostate SBRT plans were created fusing the PET/MRI imaging to computed tomography scans acquired the same day. Plans were created using only MRI-identified lesions, only PET-identified lesions, and the combined PET/MRI lesions. Coverage of the intraprostatic lesions and doses to the rectum and urethra were assessed for each of these plans.

**Results:** The majority of lesions (21/39, 53.8%) were discordant between MRI and PET, with more lesions seen by PET alone (12) than MRI alone (9). Of lesions that were concordant between PET and MRI, there were still areas that did not overlap between scans (average Dice coefficient, 0.34). Prostate SBRT planning using all lesions to define a focal intraprostatic boost provided the best coverage of all lesions without compromising constraints on the rectum and urethra.

**Conclusions:** Using both mpMRI and PSMA-directed PET may better identify all areas of gross disease within the prostate. Using both imaging modalities could improve the planning of focal intraprostatic boosts.

© 2023 The Authors. Published by Elsevier Inc. on behalf of American Society for Radiation Oncology. This is an open access article under the CC BY-NC-ND license (<http://creativecommons.org/licenses/by-nc-nd/4.0/>).

Sources of support: This study was supported with the Research and Development Pilot Grant Award (to the University of Wisconsin-Madison [UW-Madison] Radiology Department); UW Carbone Comprehensive Cancer Center Pilot Grant; and National Institutes of Health/National Cancer Institute grant 1P41EB024495-01 (Johns Hopkins University) – Service Project 2 (to UW-Madison).

Data sharing statement: Research data are stored in an institutional repository and will be shared upon request to the corresponding author.

\*Corresponding author: John M. Floberg, MD, PhD; E-mail: [jfloberg@humonc.wisc.edu](mailto:jfloberg@humonc.wisc.edu)

<https://doi.org/10.1016/j.adro.2023.101241>

2452-1094/© 2023 The Authors. Published by Elsevier Inc. on behalf of American Society for Radiation Oncology. This is an open access article under the CC BY-NC-ND license (<http://creativecommons.org/licenses/by-nc-nd/4.0/>).

## Introduction

Radiation dose escalation to gross tumor within the prostate identified on multiparametric magnetic resonance imaging (mpMRI) improves biochemical control in men with prostate cancer treated with radiation therapy (RT).<sup>1</sup> However, numerous prostate-specific membrane antigen (PSMA)-directed positron emission tomography (PET) tracers are now available and are being investigated for this purpose.<sup>2</sup>

Use of both mpMRI and PSMA PET appears to better identify prostate cancer. A recent trial demonstrated the combination of mpMRI and PSMA PET identified more clinically significant prostate cancers on biopsy than either modality alone, while also improving the negative predictive value and sensitivity; specificity was reduced.<sup>3</sup> Our own institution has conducted a trial evaluating mpMRI/PSMA PET using 2-(3-(1-carboxy-5-[(6-[<sup>18</sup>F]fluoro-pyridine-2-carbonyl)-amino]-pentyl)-ureido)-pentanedioic acid (<sup>18</sup>F-DCFPyL) in men with localized prostate cancers before undergoing radical prostatectomy (RP). PET demonstrated increased sensitivity and specificity compared with MRI, using whole-mount pathology as the reference.<sup>4</sup>

The use of both MRI and PSMA PET to define areas of disease to boost appears to be safe in patients treated with either moderately hypofractionated external beam RT or brachytherapy followed by external beam RT.<sup>2</sup> A context in which this is particularly relevant is prostate stereotactic body radiation therapy (SBRT). SBRT allows for condensed treatment and potentially delivers a higher effective dose to prostate cancer.<sup>5,6</sup> Given the high doses per fraction in prostate SBRT, feasibility and safety of boosting larger volumes of the prostate are important to define.

In this work, we first aimed to define concordance and discordance between intraprostatic lesions contoured on MRI versus PET. We did this by identifying lesions seen on one modality but not the other and by assessing the Dice and Jaccard coefficients for lesions seen on both modalities. We then aimed to determine the dosimetric feasibility of boosting disease seen on both PET and MRI with prostate SBRT in a virtual treatment planning study.

## Methods and Materials

### Patients

We used <sup>18</sup>F-DCFPyL scans from patients with localized prostate cancer enrolled on an institutional protocol investigating PET/MRI before RP.<sup>4</sup> Inclusion criteria included biopsy-proven prostate adenocarcinoma, Gleason score  $\geq 6$ ,  $>2$  biopsy cores positive, and  $\geq 7$  days post-prostate biopsy.

## Imaging

Subjects were asked to fast and hydrate for 4 to 6 hours before imaging. The <sup>18</sup>F-DCFPyL was injected via slow-intravenous push (9 mCi  $\pm$  10%). Patients underwent PET/computed tomography (CT) from skull vertex to midhigh (Discovery 710; GE Healthcare). After a 15-minute break to void, patients underwent whole-body PET/MRI (Signa; GE Healthcare). Prostate MRI was performed at 3.0 T. Sequences obtained included T2-weighted images (1.02  $\times$  0.85  $\times$  2.4 mm), diffusion-weighted images (b = 100/800 and 100/1500 s/mm<sup>2</sup>, 2.0  $\times$  2.0  $\times$  4.0 mm), and dynamic contrast-enhanced images (DISCO sequence, 25 total frames, slice thickness 4.8 mm).

## Image analysis

PET and mpMRI were reviewed concurrently by a radiation oncologist (J.M.F.), a nuclear medicine physician (S.Y.C.), and an abdominal radiologist (S.A.W.). Intraprostatic lesions were characterized as concordant or discordant between PET and MRI; lesions demonstrating any overlap between modalities were considered concordant. For concordant lesions, overlap between the PET

**Table 1** Disease characteristics of the study cohort

Characteristic	Value
Age at diagnosis, median (range)	61 (52-68)
PSA, median (range)	7.2 (3.36-20.13)
Gleason score (biopsy)	
3 + 3	3
3 + 4	6
4 + 5	4
Clinical stage	
T1c	9
T2a	2
T3c	1
T3a	1
Gleason score (prostatectomy)	
3 + 4	10
4 + 3	1
4 + 5	2
Pathologic stage	
T2	6
T3a	7
<i>Abbreviation:</i> PSA = prostate-specific antigen.	

**Table 2** Total number of, MRI detected, PET detected, concordant, and discordant intraprostatic lesions

Factor	No. (%)
Total number of lesions	39
Total MRI lesions	25
Total PET lesions	29
Total concordant lesions	18 (46.2)
Total discordant lesions	21 (53.8)
PET+ MRI–	12
MRI+ PET–	9
Average number of lesions	3.00
Average number of PET lesions	2.23
Average number of MRI lesions	1.92
Average number of concordant lesions	1.38
Average number of discordant lesions	1.62
Average PET+ MRI–	0.92
Average MRI+ PET–	0.69

*Abbreviations:* MRI = magnetic resonance imaging; PET = positron emission tomography.

and MRI contours was quantified using the Dice coefficient and Jaccard similarity coefficient, calculated in MIM (Cleveland, OH).

### Radiation treatment planning

Contouring was performed in MIM. Intraprostatic gross tumor volumes (GTVs) were identified on each imaging

modality separately and contoured with input from the radiation oncologist, nuclear medicine physician, and radiologist. MRI lesions identified as PIRADS-4 or PIRADS-5 were contoured incorporating the T2-weighted images and diffusion-weighted images. PET-identified lesions were contoured manually after windowing and leveling the PET images to visualize intraprostatic lesions relative to background activity. This is comparable with previously reported methodology, though we did not use a specific standardized uptake value range for contouring.<sup>2,7,8</sup> We did not use an automated contouring method.<sup>8,9</sup>

Contouring of the prostate, seminal vesicles, rectum, bladder, urethra, and penile bulb was performed by the radiation oncologist. The prostate and proximal 1 cm of the seminal vesicles were used as a clinical target volume and expanded by 4 mm in all directions to generate a planning target volume (PTV). No expansion was used for intraprostatic boost volumes.

Magnetic resonance and PET images were then registered to the CT obtained on the same day as the PET/MRI, and contours were transferred to the CT for SBRT planning. SBRT planning was performed in RayStation (Stockholm, Sweden). The PTV was treated to 40 Gy, with intraprostatic boost volumes treated to 45 Gy and regions of the PTV within 5 mm of the urethra, bladder, or rectum treated to 36.25 Gy (Table E1). Dose constraints are summarized in Table E2. Plans were generated boosting the GTVs contoured on MRI, PET, and both PET and MRI.

SBRT plans were characterized by quantifying coverage of the boost volumes (D95%) on each respective plan (using MRI, PET, or both). Doses to the rectum and urethra were also quantified. Measures were compared between plans using the paired Student *t* test.

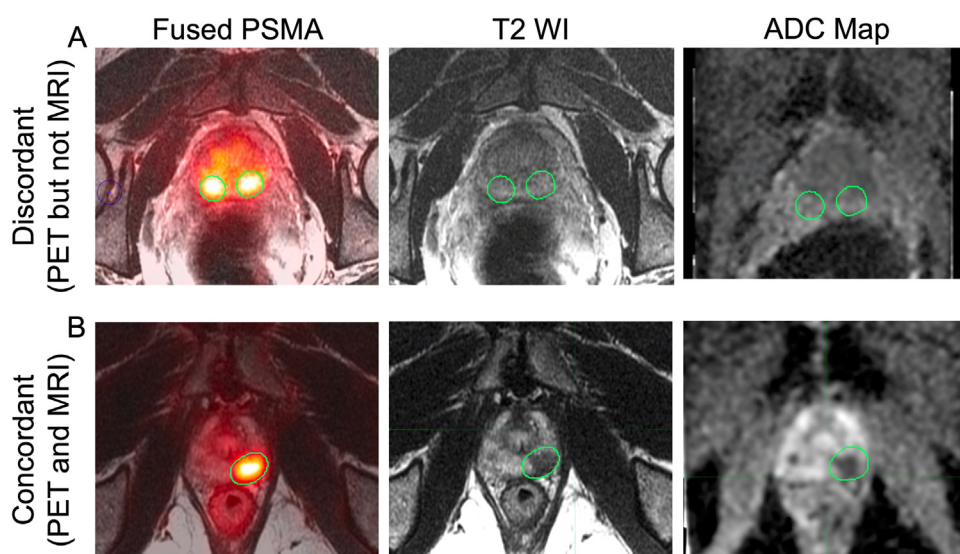


**Figure 1** PET/magnetic resonance images demonstrating a lesion seen on PET but not magnetic resonance imaging T2-weighted or diffusion sequences (A, discordant) and a lesion seen on PET, T2, and ADC (B, concordant). *Abbreviations:* ADC = apparent diffusion coefficient, PET = positron emission tomography.

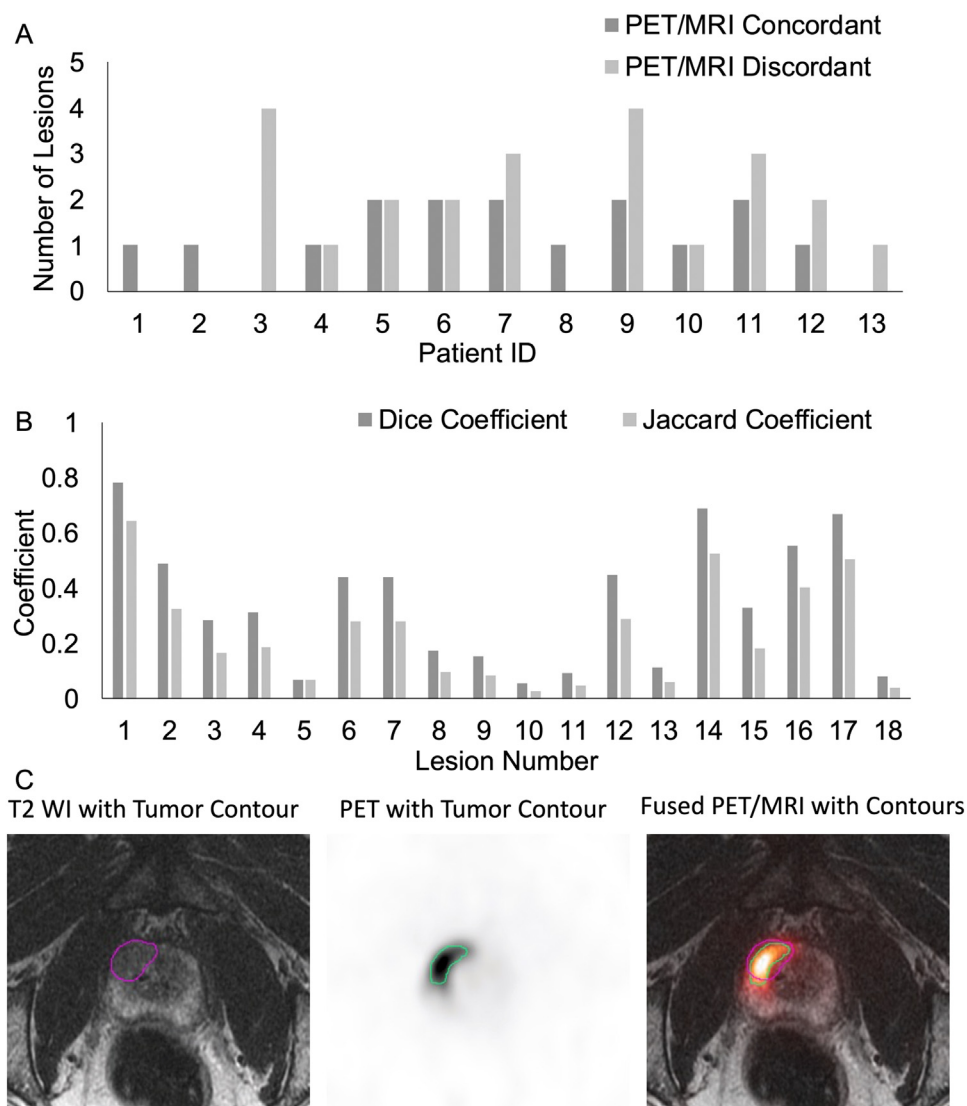


**Figure 2** The number of lesions concordant and discordant on PET and MRI for each individual patient (A). Dice and Jaccard coefficients for lesions identified as concordant between PET and MRI (B). An example lesion is shown, in which the MRI and PET identified disease overlap but are not identical (C). *Abbreviations:* MRI = magnetic resonance imaging; PET = positron emission tomography.

**Results**

Images from 13 patients were analyzed. All patients ultimately underwent radical prostatectomy. Patient characteristics are summarized in [Table 1](#).

Most patients (10/13) had more than 1 intraprostatic lesion on <sup>18</sup>F-DCFPyL PET and/or MRI. Most lesions (21/39, 53.8%) were discordant between MRI and PET. Of the discordant lesions, more were seen on PET only (12) versus MRI only (9) ([Table 2](#)). [Table E3](#) summarizes lesion locations and Gleason scores from RP specimens. Examples of discordant and concordant lesions are shown

in [Fig. 1](#). A summary of the discordant and concordant lesions per patient is shown in [Fig. 2](#).

Overlap between contours drawn on PET versus on MRI was quantified using the Dice and Jaccard similarity coefficients, summarized on a per lesion basis in [Fig. 2](#). An example lesion is also shown with contours from the T2-weighted MRI and PET. The average Dice and Jaccard similarity coefficients across all lesions were 0.34 and 0.23, respectively.

Total volume of lesions contoured on mpMRI and PET are summarized in [Table 3](#). The difference in combined mpMRI and PET volumes versus volumes from the mpMRI alone are shown in both absolute terms as well as in percent relative change.

**Table 3** Volume of mpMRI and PET GTVs, as well as the volume of the combined mpMRI and PET GTV and difference between the combined GTV and the mpMRI GTV in absolute terms (combined volume – MRI volume) and percent relative change ( $[(\text{combined volume}/\text{MRI volume}) \times 100]$ )

Patient	MRI volume (mL)	PET volume (mL)	Combined volume (mL)	Absolute difference (mL)	% Difference
1	0.98	0.9	1.14	0.16	116.3
2	0.64	1.2	1.39	0.75	217.2
3	1.09	2.35	3.45	2.36	316.5
4	1.5	2.21	3.34	1.84	222.7
5	5.62	2.52	7.84	2.22	139.5
6	2.9	3.06	4.99	2.09	172.1
7	1.82	1.74	3.32	1.5	182.4
8	0.46	4.33	4.65	4.19	1010.9
9	0.98	1.92	2.66	1.68	271.4
10	2.73	3.14	4.14	1.41	151.6
11	3.83	3.3	6.77	2.94	176.8
12	3.42	3.95	5.38	1.96	157.3
13	9.27	8.44	11.75	2.48	126.8

Abbreviations: GTV = gross tumor volume; mpMRI = multiparametric magnetic resonance imaging; MRI = magnetic resonance imaging; PET = positron emission tomography.

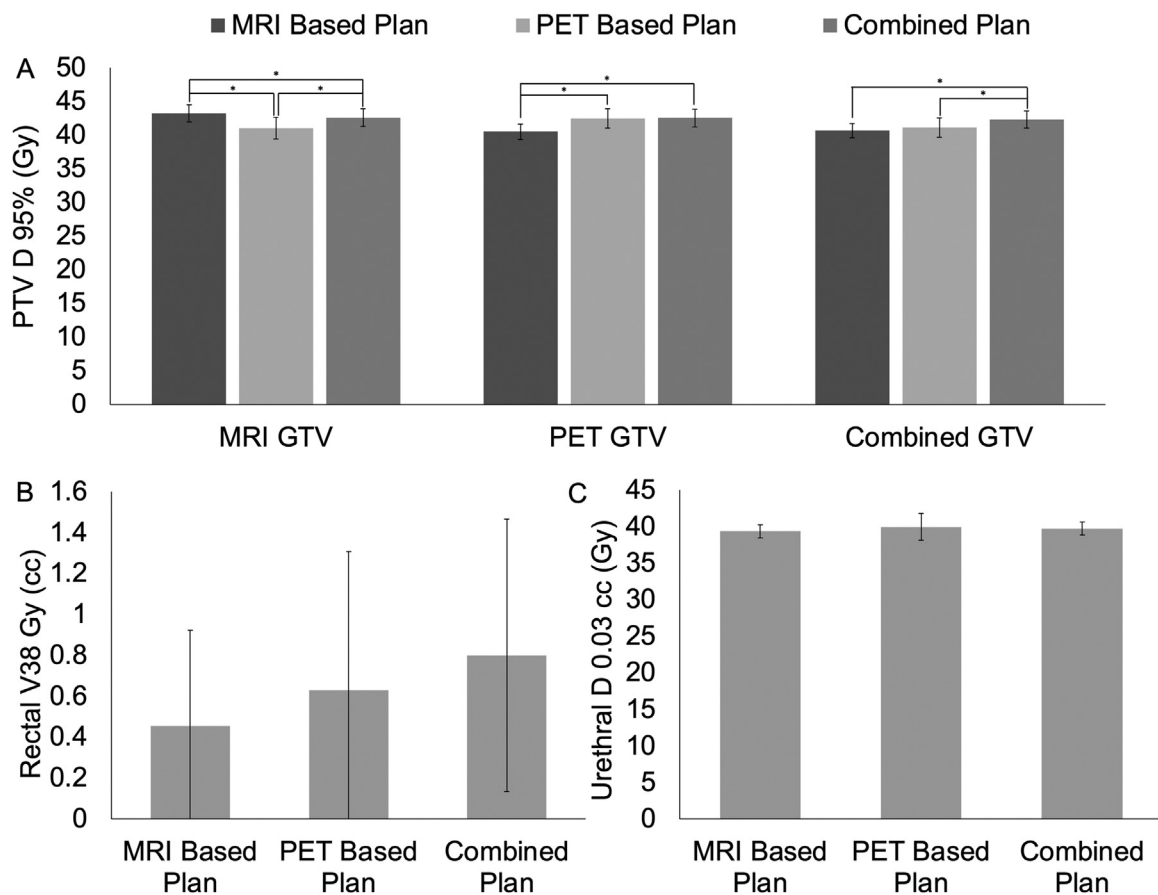


**Figure 3** Dosimetric implications of using MRI, PET, or both for intraprostatic boost planning. Target coverage for gross target volumes defined by MRI alone, PET alone, or both is shown for plans using only the MRI information, the PET information, or information from both (A). The combined plan provides the best coverage of gross target volumes defined using both MRI and PET. No significant difference was seen between the MRI-based, PET-based, or combined plans in either the dose to the rectum (B) or the dose to the urethra (C). Abbreviations: MRI = magnetic resonance imaging; PET = positron emission tomography \* =  $p < 0.05$  by the paired Student’s *t*-test.

For SBRT treatment planning, using either only MRI or PET for intraprostatic lesion contouring results in undercoverage of lesions seen on the other modality. Using both the MRI- and PET-identified disease to plan the boost leads to significantly better coverage of both PET- and MRI-defined GTVs (Fig. 3A). Although more lesions and larger volumes are used when planning with both PET and MRI, constraints were still met. Doses to the rectum (V38 Gy) and urethra (D0.03 cc) were not significantly different between the MRI-based, PET-based, or combined plans (Fig. 3B, 3C).

## Discussion

Use of a simultaneous RT boost to gross disease within the prostate defined by mpMRI is supported by randomized data.<sup>1</sup> However, PSMA PET combined with mpMRI may better identify gross areas of tumor,<sup>3</sup> and use of both modalities to plan intraprostatic boosts is being prospectively studied.<sup>2,7,10</sup> This current study is unique in that it used simultaneously acquired PET/MRI scans, limiting misregistration of images acquired at different times, and it used <sup>18</sup>F-DCFPyL, a tracer commercially available in the United States.

This study supports the use of both mpMRI and <sup>18</sup>F-DCFPyL PET for planning intraprostatic boosts for prostate SBRT. Lesions contoured only with MRI or PET do not capture the full extent of disease (Figs. 2 and 3, Table 1). It is important to note that although PET and mpMRI were acquired simultaneously, some discrepancies from registration inaccuracies are inevitable due to motion of the patient or organs during the scans. For SBRT treatment planning, using only MRI or PET for contouring GTVs results in undercoverage of the lesions identified on the other modality. We notably have not made any comparison with the radical prostatectomy specimens in this work; this is being reported separately.<sup>4</sup> Regardless, careful consideration must be given as to which lesions to boost—ideally those also with pathologic confirmation from biopsy—as both PET and MRI can produce false positives.

There are several limitations of this study. The specificity of both mpMRI and PSMA PET tracers is limited.<sup>3,11–14</sup> Though some of this is inherent to the imaging modalities, there are some key physiological and anatomic considerations. Imaging close to a prostate biopsy can affect both mpMRI and potentially PSMA PET because of the presence of blood products. Location of a lesion within the prostate can also affect accuracy of mpMRI and PSMA PET.<sup>15–18</sup> These factors should be further explored.

Another consideration is that this study used <sup>18</sup>F-DCFPyL. This is distinct from the PRIMARY and HypoFocal trials, which used <sup>68</sup>Ga-PSMA-11 or <sup>18</sup>F-PSMA-1007.<sup>3,7</sup> <sup>18</sup>F-DCFPyL has been well described and its diagnostic performance is similar to that of <sup>68</sup>Ga-PSMA-11.<sup>19–22</sup> However,

any given tracer will have differences in pharmacokinetics and thus will also have differences in quantitative metrics and the signal of tumor versus surrounding structures.

## Conclusion

These data suggest that a more complete picture of total gross intraprostatic cancer is obtained with the combination of both MRI and PSMA-based PET. Both modalities could be used for SBRT planning if using an intraprostatic boost to gross disease.

## Disclosures

Dr Morris reports the following conflicts of interest: Archeus Technologies, scientific advisory board; Seneca Therapeutics, scientific advisory board.

Dr Wells reports the following conflicts of interest: Ethicon, consultant. Dr Cho reports the following conflicts of interest: Progenics Pharmaceuticals, consultant. No other disclosures were reported.

## Supplementary materials

Supplementary material associated with this article can be found in the online version at doi:10.1016/j.adro.2023.101241.

## References

- Kerkmeijer LGW, Groen VH, Pos FJ, et al. Focal boost to the intraprostatic tumor in external beam radiotherapy for patients with localized prostate cancer: Results from the FLAME randomized phase III trial. *J Clin Oncol*. 2021;39:787–796.
- Zamboglou C, Spohn SKB, Ruf J, et al. PSMA-PET- and MRI-based focal dose escalated radiation therapy of primary prostate cancer: Planned safety analysis of a nonrandomized 2-armed phase 2 trial (ARO2020-01). *Int J Radiat Oncol Biol Phys*. 2022;113:1025–1035.
- Emmett L, Buteau J, Papa N, et al. The additive diagnostic value of prostate-specific membrane antigen positron emission tomography computed tomography to multiparametric magnetic resonance imaging triage in the diagnosis of prostate cancer (PRIMARY): A prospective multicentre study. *Eur Urol*. 2021;80:682–689.
- Lee CL, Wells S, Huang W, Jarrard D, Cho S. Radiology-pathology correlation of <sup>18</sup>F-DCFPyL PSMA PET and multi-parametric prostate MRI in men with prostate cancer. *J Nucl Med*. 2022;63(suppl 2):2545.
- Bentzen SM, Ritter MA. The alpha/beta ratio for prostate cancer: What is it, really? *Radiother Oncol*. 2005;76:1–3.
- Vogelius IR, Bentzen SM. Meta-analysis of the alpha/beta ratio for prostate cancer in the presence of an overall time factor: Bad news, good news, or no news? *Int J Radiat Oncol Biol Phys*. 2013;85:89–94.
- Zamboglou C, Spohn SKB, Adebahr S, et al. PSMA-PET/MRI-based focal dose escalation in patients with primary prostate cancer treated with stereotactic body radiation therapy (hypofocal-SBRT): Study

- protocol of a randomized, multicentric phase III trial. *Cancers (Basel)*. 2021;13:5795.
8. Zamboglou C, Fassbender TF, Steffan L, et al. Validation of different PSMA-PET/CT-based contouring techniques for intraprostatic tumor definition using histopathology as standard of reference. *Radiother Oncol*. 2019;141:208-213.
  9. Draulans C, De Roover R, van der Heide UA, et al. Optimal <sup>68</sup>Ga-PSMA and <sup>18</sup>F-PSMA PET window levelling for gross tumour volume delineation in primary prostate cancer. *Eur J Nucl Med Mol Imaging*. 2021;48:1211-1218.
  10. Spohn SKB, Adebahr S, Huber M, et al. Feasibility, pitfalls and results of a structured concept-development phase for a randomized controlled phase III trial on radiotherapy in primary prostate cancer patients. *BMC Cancer*. 2022;22:337.
  11. de Rooij M, Hamoen EH, Fütterer JJ, Barentsz JO, Rovers MM. Accuracy of multiparametric MRI for prostate cancer detection: A meta-analysis. *AJR Am J Roentgenol*. 2014;202:343-351.
  12. Bass EJ, Pantovic A, Connor M, et al. A systematic review and meta-analysis of the diagnostic accuracy of biparametric prostate MRI for prostate cancer in men at risk. *Prostate Cancer Prostatic Dis*. 2021; 24:596-611.
  13. Ahmed HU, El-Shater Bosaily A, Brown LC, et al. Diagnostic accuracy of multi-parametric MRI and TRUS biopsy in prostate cancer (PROMIS): A paired validating confirmatory study. *Lancet*. 2017;389:815-822.
  14. Pienta KJ, Gorin MA, Rowe SP, et al. A phase 2/3 prospective multicenter study of the diagnostic accuracy of prostate specific membrane antigen PET/CT with <sup>18</sup>F-DCFPyL in prostate cancer patients (OSPREY). *J Urol*. 2021;206:52-61.
  15. Merisaari H, Jambor I, Ettala O, et al. Improd biparametric MRI in men with a clinical suspicion of prostate cancer (IMPROD trial): Sensitivity for prostate cancer detection in correlation with whole-mount prostatectomy sections and implications for focal therapy. *J Magn Reson Imaging*. 2019;50:1641-1650.
  16. Park KJ, Choi SH, Kim MH, Kim JK, Jeong IG. Performance of prostate imaging reporting and data system version 2.1 for diagnosis of prostate cancer: A systematic review and meta-analysis. *J Magn Reson Imaging*. 2021;54:103-112.
  17. Ginsburg SB, Algohary A, Pahwa S, et al. Radiomic features for prostate cancer detection on MRI differ between the transition and peripheral zones: Preliminary findings from a multi-institutional study. *J Magn Reson Imaging*. 2017;46:184-193.
  18. Ganeshalingam R, Hsiao E. Compressed central zone uptake on PSMA PET/CT: A potential pitfall in interpretation. *Clin Nucl Med*. 2019;44:570-571.
  19. Szabo Z, Mena E, Rowe SP, et al. Initial evaluation of [(18)F] DCFPyL for prostate-specific membrane antigen (PSMA)-targeted PET imaging of prostate cancer. *Mol Imaging Biol*. 2015;17:565-574.
  20. Morris MJ, Rowe SP, Gorin MA, et al. Diagnostic performance of <sup>18</sup>F-DCFPyL-PET/CT in men with biochemically recurrent prostate cancer: results from the CONDOR phase III, multicenter study. *Clin Cancer Res*. 2021;27:3674-3682.
  21. Dietlein M, Kobe C, Kuhnert G, et al. Comparison of [(18)F] DCFPyL and [(68)Ga]Ga-PSMA-HBED-CC for PSMA-PET imaging in patients with relapsed prostate cancer. *Mol Imaging Biol*. 2015;17:575-584.
  22. Dietlein F, Kobe C, Neubauer S, et al. PSA-stratified performance of <sup>18</sup>F- and <sup>68</sup>Ga-PSMA PET in patients with biochemical recurrence of prostate cancer. *J Nucl Med*. 2017;58:947-952.